Photosynthetic Complex LH2 (B850 and B800 Ring) - Static Disorder in Radial Positions of Molecules

PAVEL HEŘMAN
Department of Physics
Faculty of Science
University of Hradec Králové
Rokitanského 53, Hradec Králové
CZECH REPUBLIC
pavel.herman@uhk.cz

DAVID ZAPLETAL
Institute of Mathematics and Quant. Methods
Faculty of Economy and Administration
University of Pardubice
Studentská 95, Pardubice
CZECH REPUBLIC
david.zapletal@upce.cz

Abstract: - Light–harvesting (LH) pigment–protein complexes interact with their environment, which strongly influences their properties. Slow fluctuations of environment could be modeled by different types of static disorder. LH2 complex from purple bacteria is investigated in present paper. This complex consists of two bacteriochlorophyll rings (B850 ring and B800 ring). Distributions of the nearest neighbour transfer integrals in B800 ring and the nearest neighbour transfer integrals connecting B850 and B800 ring are presented. The most important statistical properties are calculated, discussed and compared in case of uncorrelated static disorder in radial positions of bacteriochorophyll molecules.

Key-Words: - B800 ring, B850 ring, LH2 complex, Hamiltonian, static disorder, transfer integral distributions

1 Introduction

Some organisms, e.g. green plants, bacteria, blue–green algae, etc., have ability to transform energy of light into chemical energy. This process is called photosynthesis. Photosynthesis could be divided to two stages (light stage and dark stage). The first (light) stage consists of photochemical reactions. Light photon is absorbed and a series of electron transfers is driven by its energy. As the result, adenosine triphosphate (ATP) and nicotine adenine dinucleotide phosphate (NADPH – reduced form) are synthesized. Then, the ATP and NADPH are used for reduction of carbon dioxide to organic carbon compounds during the dark stage [1].

Researchers have been focused on investigation of photosynthesis for a long time. Our research is concerned the light stage of photosynthesis in purple bacteria. Absorption of solar photons by a complex system of membrane–associated pigment–proteins (light–harvesting (LH) antenna) gives excitation energy (in the form of Frenkel excitons). Then efficient transfer to a reaction center occurs. There excitons are converted into a chemical energy [2].

Geometric structures of photosynthetic complexes from purple bacteria are known in great detail from X–ray crystallography. Their antenna systems are arranged as ring units. A ring–shaped structure is formed by cyclic repetition of identical subunits. The organization of these LH complexes is generally the same, but their symmetry can be different.

Crystal structure of peripheral LH2 complex contained in purple bacterium Rhodopseudomonas acidophila was described by McDermott et al. [3] and then further e.g. Papiz et al. [4]. Two concentric rings (B850 ring and B800 one) are created by bacteriochlorophyll (BChl) molecules. Eighteen closely packed BChl molecules are arranged in B850 ring (with absorption band at about 850 nm). B800 ring consists of nine well–separated BChl molecules absorbing around 800 nm. Organization of the whole LH2 complex is nonameric, i.e. it consists of nine identical subunits. Dipole moments of BChl molecules are oriented approximately tangentially to the ring. Arrangement of LH2 complexes from other purple bacteria is analogous.

Also other types of peripheral light–harvesting complexes can be found in some purple bacteria (B800–820 LH3 complex in Rhodopseudomonas acidophila strain 7050 or LH4 complex in Rhodopseudomonas palustris). LH3 complex like LH2 one is usually nonameric [5]. LH4 complex consists of eight identical subunits, i.e. it is octameric, and it consists of three concentric BChl rings [6]. Light harvesting complexes can also differ in orientations of BChl dipole moments and consequently in strengths of mutual interactions between BChl molecules. For instance, BChl dipole moments in B–α/B–β ring from LH4 complex are oriented approximately radially to the ring. Interactions between the nearest neighbour BChls in B–α/B–β ring are approximately two times weaker in comparison with B850 ring from LH2 complex and they have opposite sign.

Purple bacteria contain (beside peripheral antenna complexes) also core antenna complexes that include reaction centers (RC). For instance LH1 complex from Rhodopseudomonas acidophila consists of approximately 16 structural subunits in which two BChl molecules are noncovalently attached to pairs of transmembrane polypeptides. These subunits again have ring like structure which surrounds RC [7].

The intermolecular distances under 1 nm imply strong exciton couplings between corresponding BChl molecules. Therefore an extended Frenkel exciton states model can be applied in theoretical approach. The solvent and protein environment of BChl rings fluctuates. Characteristic time scale of these fluctuations at room temperature have range from femtoseconds to nanoseconds. Fast fluctuations can be modeled by dynamic disorder and slow fluctuations by static disorder. Influence of static disorder in local excitation energies on the anisotropy of fluorescence for LH2 complexes was studies by Kumble and Hochstrasser [8] and Nagarajan et al. [9,10]. We extended these investigations by addition of dynamic disorder (simple model systems [11–13], models of B850 ring (from LH2) [14,15]). We also consider various types of uncorrelated static disorder and correlated one (e.g., elliptical deformation) [16–18]. Comparison of the results for B850 ring from LH2 complex and B–α/B–β ring from LH4 complex, that have different arrangements of optical dipole moments, was also done [19–22]. Recently, our investigation has been focused on the modeling of absorption and fluorescence spectra of LH2 and LH4 complexes within the nearest neighbor approximation model [23–27] and full Hamiltonian model [28–36].

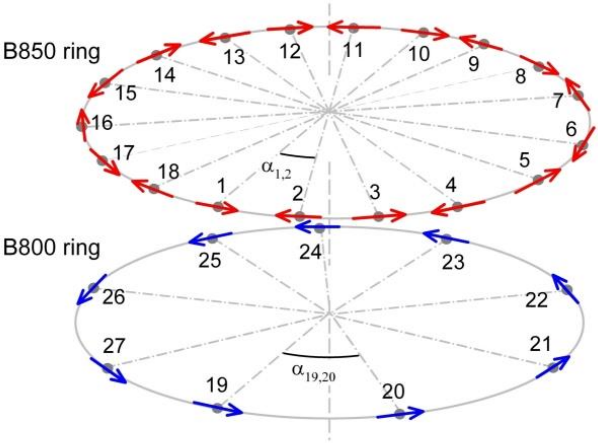

Fig. 1: Geometric arrangement of ideal LH2 complex without any fluctuations – dipole moments are oriented tangentially to the rings (B850 ring: $\alpha_{m,\mathrm{m}+1} = \pi/9$, dipole moments – red arrows; B800 ring $\alpha_{m,\mathrm{m}+1} = 2\pi/9$, dipole moments – blue arrows)

Very recently we have started to investigate the nearest neighbour transfer integral distributions for various types of static disorder connected with fluctuations in ring geometry of B850 ring from LH2 complex [37-39]. Main goal of the present paper is the extension of this investigation to the whole LH2 complex (B850 ring and B800 one). The rest of the paper is structured as follows. Section 2 introduces the ring model with different types of static disorder. Used units and parameters can be found in Section 3. Results are presented and discussed in Section 4 and conclusions are drawn in Section 5.

2 Model

We consider only one exciton on molecular complex, e.g. LH2 complex. Then Hamiltonian of the exciton consists of four terms in our model:

$$H = H_{\mathrm{ex}}^0 + H_{\mathrm{s}} + H_{\mathrm{ph}} + H_{\mathrm{ex\text{-}ph}}. \qquad (1)$$

2.1 Ideal Molecular Complex

The first term in Eq. (1),

$$H_{\mathrm{ex}}^0 = \sum_{m=1}^{N} E_m^0 a_m^\dagger a_m + \sum_{m,n=1(\mathrm{m}\neq\mathrm{n})}^{N} J_{m,n}^0 a_m^\dagger a_n, \qquad (2)$$

describes an exciton on the ideal ring, i.e. without any disorder. Here $a_m^\dagger$ (a_m) are creation (annihilation) operators of an exciton at site m, E_m^0 is the local excitation energy of m–th molecule, $J_{m,n}^0$ (for $m \neq n$) is the so–called transfer integral between sites m and n. N is the number of molecules in our system (N=27). Local excitation energies E_m^0 are the same for all BChls in our molecular complex, i.e.

$$E_m^0 = E_0, \quad m = 1,\ldots,N. \qquad (3)$$

Whole LH2 complex (without any disorder) has nine fold symmetry (see Fig.1). That is why, the interaction strengths between BChls in B850 ring fulfil condition:

$$J_{m,n}^0 = J_{m+2i,n+2i}^0, \qquad (4)$$

where

$$m, n, m+2i, n+2i = 1, \ldots, 18.$$

Equivalent condition holds for the interaction strengths in B800 ring:

$$J^0_{m,n} = J^0_{m+i,n+i}, \qquad (5)$$

$$m, n, m+i, n+i = 19, \ldots, 27.$$

For the strengths of remaining interactions (one molecule is from B850 ring and one from B800 ring) can be written:

$$J^0_{m,n} = J^0_{m+2i,n+i}, \qquad (6)$$

$$m, m+2i = 1, \ldots, 18, \quad n, n+i = 19, \ldots, 27.$$

In what follows only interactions between nearest neighbour BChl molecules are consider to be nonzero, i.e. the nearest neighbour approximation is used. The interaction strengths $J^0_{1,2}$ and $J^0_{2,3}$ between the nearest neighbour BChls inside ideal B850 ring are almost the same (see Fig.1 (B) in [6]). Such ring can be modeled as homogeneous case,

$$J^{0(\mathrm{B850})}_{m,n} = J_0(\delta_{m,n+1} + \delta_{m,n-1}), \qquad (7)$$

$$m, n, n+1, n-1 = 1, \ldots, 18.$$

Analogous property can be found for B800 ring,

$$J^{0(\mathrm{B800})}_{m,n} = J_0(\delta_{m,n+1} + \delta_{m,n-1}), \qquad (8)$$

$$m, n, n+1, n-1 = 19, \ldots, 27.$$

Transfer integrals $J_{m,n}$ in dipole–dipole approximation read

$$J_{m,n} = \frac{\vec{d}_m \cdot \vec{d}_n}{|\vec{r}_{mn}|^3} - 3\frac{(\vec{d}_m \cdot \vec{r}_{mn})(\vec{d}_n \cdot \vec{r}_{mn})}{|\vec{r}_{mn}|^5} =$$

$$= |\vec{d}_m||\vec{d}_n| \frac{\cos\varphi_{mn} - \cos\varphi_m \cos\varphi_n}{|\vec{r}^{\,3}_{mn}|}. \qquad (9)$$

Here local dipole moments of m–th and n–th molecule are denoted as $\vec{d}_m$ and $\vec{d}_n$, the angle between these dipole moment vectors (d_m, d_n) is referred to as φ_{mn}. Vector $\vec{r}_{mn}$ connects m–th and n–th molecule, φ_m (φ_n) symbolizes the angle between $\vec{d}_m$ ($\vec{d}_n$) and $\vec{r}_{mn}$. In case of ideal molecular complex LH2 (without any disorder) the distances $\vec{r}_{m,m+1}$ of neighbouring BChl molecules are the same as in B850 ring as in B800 one. Therefore angles $\beta_{m,m+1}$ have to be the same too $\beta_{m,m+1} = 2\pi/18$, see Fig.1), i.e.

$$\beta_{m,m+1} = \frac{\pi}{9} \qquad (10)$$

in B850 ring and

$$\beta_{m,m+1} = \frac{2\pi}{9} \qquad (11)$$

in B800 ring.

Due to orientations of dipole moments (see Figure 1), sign of J_0 is positive, sign of J_0 is negative and the relation between them is given by the following equation:

$$J_1 = -0.1 J_0. \qquad (12)$$

As concerns transfer integrals connecting B850 ring and B800 one, each BChl from B800 ring is connected by nonzero transfer integrals with two nearest neighbour BChls from B850 ring. These transfer integrals have opposite signs. Their values are

$$J_{1,19} = J_{3,20} = \ldots = J_{17,27} = 0.1 J_0, \qquad (13)$$

$$J_{2,19} = J_{4,20} = \ldots = J_{18,27} = -0.03 J_0. \qquad (14)$$

The values of these nearest neighbour transfer integrals (J_0, J_1, $J_{1,19}$, $J_{2,19}$) determine the geometric structure of LH2 complex.

2.2 Static Disorder

The second term in Eq. (1), Hs, corresponds to static disorder. One of the ways to take into account such disorder is to model it as slow fluctuations in ring geometry. Deviation in ring geometry results in changes of transfer integrals $\delta J_{m,n}$,

$$J_{m,n} = J_{n,m} = J^0_{m,n} + \delta J_{m,n}. \qquad (15)$$

Static disorder in ring geometry can be consider in two ways – fluctuations in molecular positions or fluctuations in molecular dipole moment orientations. We studied both types of fluctuations but only in the B850 ring [37-39]. In the present paper we consider the whole LH2 complex (including as B850 ring as B800 one) and the first above mentioned type of static disorder – fluctuations in molecular positions. The simplest model of such fluctuations is to have nonzero only changes of radial positions of molecules in both rings. Then we have

$$r_m = r_0 + \delta r_m, \qquad m = 1, \ldots, 18 \qquad (16)$$

in B850 ring (r_0 is the diameter of unperturbed B850 ring) and

$$r_m = r_1 + \delta r_m, \qquad m = 19, \ldots, 27. \qquad (17)$$

in B800 ring (r_1 is the diameter of unperturbed B800 ring). The axial distance of B850 ring and B800 one and the angles $\alpha_{m,n}$ remain the same as in ideal LH2 complex (see Fig.1). Due to the consideration of dipole–dipole approximation the connection between fluctuations of geometry and fluctuations of transfer integrals is given by Eq. (9).

2.2 Dynamic Disorder

Finally, the third and fourth term in Eq (1), H_{ph} and $H_{\mathrm{ex\text{-}ph}}$ represents dynamic disorder, i.e. phonon bath and exciton–phonon interaction which is supposed to be local and linear in bath coordinates. We consider only static disorder in this paper and neglect these terms.

3 Units and Parameters

Dimensionless energies normalized to the transfer integral $J^0_{m,m+1} = J_0$ in B850 ring (see Eq. (12)) have been used in our calculations. Estimation of J_0 varies in literature between 250 cm^{-1} and 400 cm^{-1}. In our previous investigations [40] we found (from comparison with experimental results for B850 ring from the LH2 complex [41]) that the possible strength Δ_J of the uncorrelated Gaussian static disorder δJ_{mn} in transfer integrals is approximately $\Delta_J \approx 0.15 J_0$. The strength of above mentioned type of static disorder in ring geometry is taken in connection with the strength Δ_J. That is why we have taken the strength Δ_r for our type of static disorder in following interval:

$$\Delta_r \in \langle 0.02 r_0, 0.30 r_0 \rangle. \qquad (18)$$

All our calculations were done for 20000 realizations of static disorder.

4 Results and Discussion

Fluctuations in radial positions of molecules strongly influence Hamiltonian of LH2 complex. Distributions of the nearest neighbour transfer transfer integrals for the whole LH2 complex (in B850 ring, B800 one and also transfer integrals connecting both rings) were calculated for above mentioned static disorder type. Graphical presentation of these distributions is done by contour plots and line plots in Fig.2 – Fig.5. Values of $E(J)$ and $E(J) \pm \sqrt{D(J)}$ for these distributions are also included in contour plots. Here $E(J)$ is sample expected value,

$$E(J) = \frac{1}{n} \sum_{i=1}^{n} J_i, \qquad (19)$$

and $\sqrt{D(J)}$ is sample standard deviation,

$$\sqrt{D(J)} = \sqrt{\frac{1}{n-1} M_2}. \qquad (20)$$

In addition, sample skewness α_3,

$$\alpha_3 = \frac{n^{\frac{5}{2}}}{(n-1)(n-2)} \frac{M_3}{M_2^{\frac{3}{2}}}, \qquad (21)$$

and sample kurtosis α_4,

$$\alpha_4 = \frac{n^2}{(n-2)(n-3)} \left[\frac{n(n+1)}{n-1} \frac{M_4}{M_2^2} - 3 \right], \qquad (22)$$

were calculated. Here M_k, which is given by

$$M_k = \sum_{i=1}^{n} \left[J_i - E(J) \right]^k, \qquad (23)$$

denotes *k*–th central moment and *n* is the number of cases in our samples. Also sample coefficient of variation *c* was calculated,

$$c = \frac{\sqrt{D(J)}}{E(J)}. \qquad (24)$$

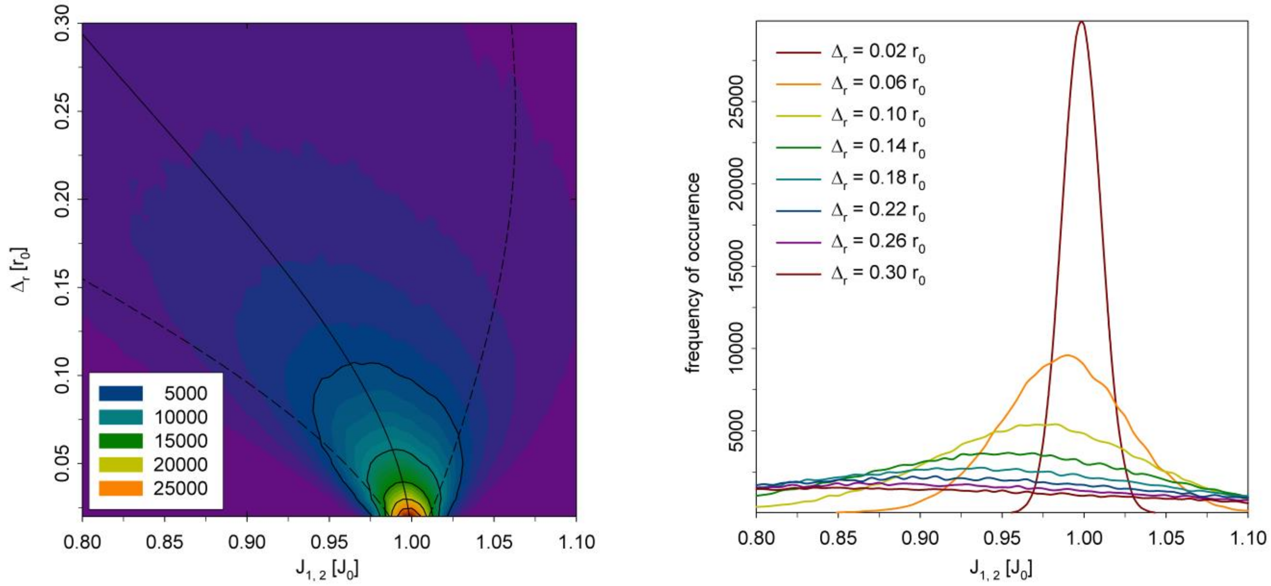

Fig.2: Distributions of the nearest neighbour transfer integrals $J_{1,2}, J_{2,3}, \ldots, J_{18,1}$ connecting the nearest neighbour BChl molecules in B850 ring – uncorrelated Gaussian static disorder $\delta r_m (m = 1, \ldots, 27)$ in radial positions of BChl molecules; the strength of static disorder $\Delta_r \in \langle 0.02 r_0, 0.30 r_0 \rangle$.

Strength of disorder Δ_r	Expected value $E(J)$	Standard deviation $\sqrt{D(J)}$	Skewness α_3	Kurtosis α_4	Coefficient of variation c
$0.02\, r_0$	0.999	0.012	0.045	-0.002	0.012
$0.06\, r_0$	0.988	0.039	-0.092	0.318	0.039
$0.10\, r_0$	0.967	0.073	-0.349	0.886	0.075
$0.14\, r_0$	0.939	0.112	-0.489	1.060	0.119
$0.18\, r_0$	0.905	0.153	-0.497	0.872	0.169
$0.22\, r_0$	0.869	0.193	-0.422	0.567	0.222
$0.26\, r_0$	0.832	0.231	-0.304	0.291	0.278
$0.30\, r_0$	0.794	0.266	-0.165	0.102	0.335

Table 1: Expected value, standard deviation, skewness, kurtosis and coefficient of variation for the distributions of the nearest neighbour transfer integrals $J_{1,2}, J_{2.3}, \ldots, J_{18,1}$ connecting B850 ring and B800 one – uncorrelated Gaussian static disorder δr_m (m=1,…,27) in radial positions of BChl molecules (eight strengths Δ_r of static disorder).

Table 1 - Table 4 contain the values of sample characteristics $E(J)$, $\sqrt{D(J)}$, α_3, α_4 and c (see Eq.(19) – Eq.(24)) for chosen static disorder strengths. Our results were calculated from 20000 realizations of static disorder and due to the number of bacteriochlorophylls in B800 ring the number of cases n in our samples equals 180000.

If we consider Gaussian distribution of molecular radial positions, resulting distributions of the nearest neighbour transfer integrals are non–Gaussian. From Fig.2 - Fig.5 and Table 1 - Table 4 it is clear that the expected values $E(J)$ are non–constant (except $J_{2,19}$). On the other hand, Gaussian distribution of transfer integrals has constant expected value and standard deviation equals the strength of static disorder $\sqrt{D(J)} = \Delta_J$. The level of deviation from Gaussian distribution can also be assessed through

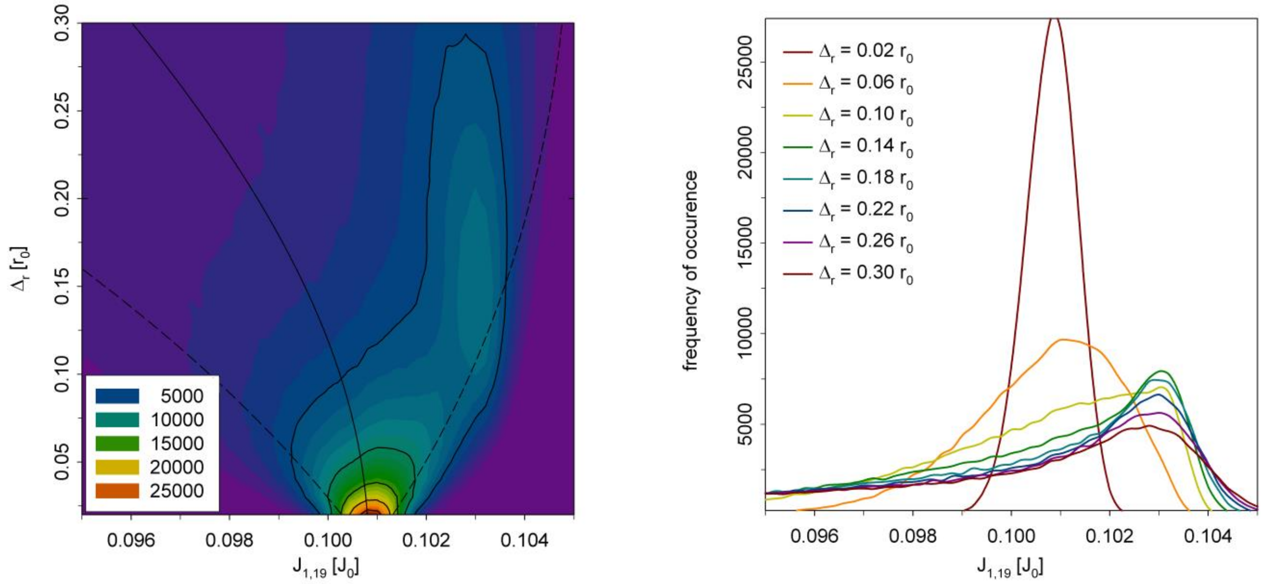

Fig.3 Distributions of the nearest neighbour transfer integrals $J_{1,19}, J_{3,20}, \ldots, J_{17,27}$ connecting BChl molecules in B850 ring and B800 one – uncorrelated Gaussian static disorder $\delta r_m (m = 1, \ldots, 27)$ in radial positions of BChl molecules; the strength of static disorder $\Delta_r \in \langle 0.02 r_0, 0.30 r_0 \rangle$

Strength of disorder Δ_r	Expected value $E(J)$	Standard deviation $\sqrt{D(J)}$	Skewness α_3	Kurtosis α_4	Coefficient of variation c
0.02 r_0	0.101	0.001	-0.270	0.092	0.005
0.06 r_0	0.101	0.002	-0.777	0.743	0.016
0.10 r_0	0.100	0.003	-1.190	1.728	0.026
0.14 r_0	0.100	0.004	-1.481	2.650	0.038
0.18 r_0	0.099	0.005	-1.655	3.262	0.050
0.22 r_0	0.098	0.006	-1.735	3.509	0.063
0.26 r_0	0.097	0.007	-1.748	3.459	0.077
0.30 r_0	0.096	0.009	-1.716	3.214	0.091

Table 2: Expected value, standard deviation, skewness, kurtosis and coefficient of variation for the distributions of the nearest neighbour transfer integrals $J_{1,19}, J_{3.20}, \ldots, J_{17,27}$ connecting BChl molecules B850 ring and B800 one – uncorrelated Gaussian static disorder δr_m (*m*=1,…,27) in radial positions of BChl molecules (eight strengths Δ_r of static disorder).

the skewness α_3 and the kurtosis α_4. These characteristics are also nonconstant (contrary, $\alpha_3 = \alpha_4 = 0$ for Gaussian distribution). As concerns expected value $E(J)$, if the static disorder strength Δ_r increases, $E(J)$ decreases for the distribution of $J_{1,2}$ and $J_{1,19}$ and it increases for $J_{19,20}$. Only for the distribution of $J_{2,19}$ the expected value is nearly constant. As the signs of $J_{1,2}$, $J_{1,19}$ and $J_{19,20}$ are different, absolute values of $E(J)$ decrease in all three cases. All four distributions of $J_{1,2}$, $J_{1,19}$, $J_{2,19}$ and $J_{19,20}$ are negatively skewed (to the left hand side) (see Fig.2 – Fig.5). It corresponds with negative

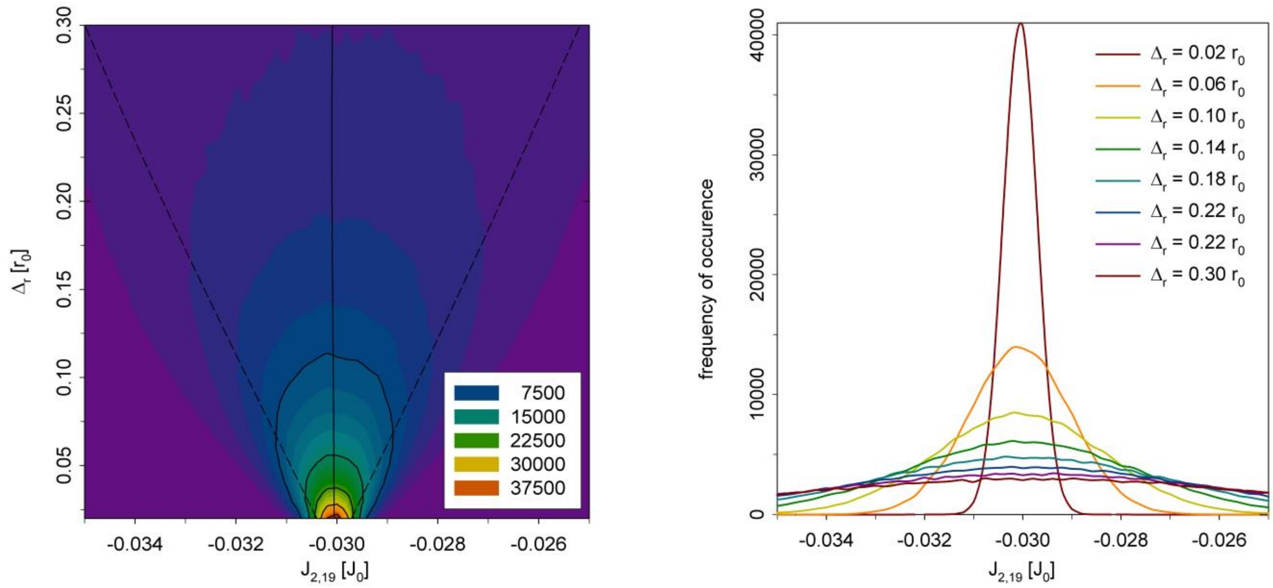

Fig.4 Distributions of the nearest neighbour transfer integrals $J_{2,19}, J_{4,20}, \ldots, J_{18,27}$ connecting BChl molecules in B850 ring and B800 one – uncorrelated Gaussian static disorder $\delta r_m (m=1, \ldots, 27)$ in radial positions of BChl molecules; the strength of static disorder $\Delta_r \in \langle 0.02 r_0, 0.30 r_0 \rangle$

Strength of disorder Δ_r	Expected value $E(J)$	Standard deviation $\sqrt{D(J)}$	Skewness α_3	Kurtosis α_4	Coefficient of variation c
$0.02\, r_0$	-0.030	0.000	-0.006	0.010	-0.011
$0.06\, r_0$	-0.030	0.001	-0.021	0.013	-0.034
$0.10\, r_0$	-0.030	0.002	-0.038	0.018	-0.057
$0.14\, r_0$	-0.030	0.002	-0.056	0.027	-0.079
$0.18\, r_0$	-0.030	0.003	-0.075	0.040	-0.101
$0.22\, r_0$	-0.030	0.004	-0.097	0.056	-0.122
$0.26\, r_0$	-0.030	0.004	-0.121	0.075	-0.143
$0.30\, r_0$	-0.030	0.005	-0.147	0.097	-0.163

Table 3: Expected value, standard deviation, skewness, kurtosis and coefficient of variation for the distributions of the nearest neighbour transfer integrals $J_{2,19}, J_{4,20}, \ldots, J_{18,27}$ connecting BChl molecules B850 ring and B800 one – uncorrelated Gaussian static disorder δr_m (m=1,…,27) in radial positions of BChl molecules (eight strengths Δ_r of static disorder).

values of sample skewness α_3. The dependences of α_3 on Δ_r show nonlinearity in case of $J_{1,2}$ and $J_{1,19}$ and they are approximately linear for $J_{2,19}$ and $J_{19,20}$ increasing static disorder strength Δ_r in case of the (see Fig.6). Sample kurtosis α_4 increases with distribution of $J_{2,19}$ and $J_{19,20}$. The dependences of α_4 on Δ_r are more complicated for the distributions of $J_{1,2}$ and $J_{1,19}$. The kurtosis increases for lower Δ_r and decreases for upper Δ_r with maximum in our

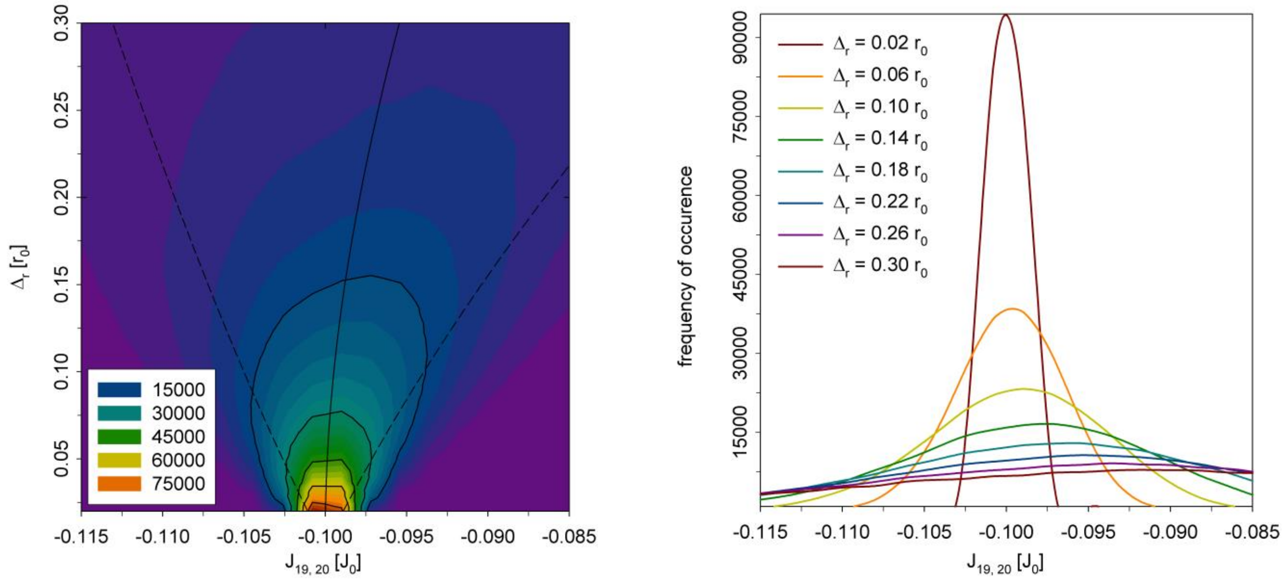

Fig.5 Distributions of the nearest neighbour transfer integrals $J_{19,20}, J_{20,21}, \ldots, J_{27,19}$ connecting the nearest neighbour BChl molecules in B800 ring – uncorrelated Gaussian static disorder $\delta r_m (m = 1, \ldots, 27)$ in radial positions of BChl molecules; the strength of static disorder $\Delta_r \in \langle 0.02 r_0, 0.30 r_0 \rangle$.

Strength of disorder Δ_r	Expected value $E(J)$	Standard deviation $\sqrt{D(J)}$	Skewness α_3	Kurtosis α_4	Coefficient of variation c
0.02 r_0	-0.100	0.001	-0.046	0.000	-0.011
0.06 r_0	-0.100	0.003	-0.132	0.032	-0.033
0.10 r_0	-0.099	0.006	-0.211	0.094	-0.056
0.14 r_0	-0.099	0.008	-0.281	0.185	-0.079
0.18 r_0	-0.098	0.010	-0.345	0.305	-0.104
0.22 r_0	-0.097	0.013	-0.404	0.449	-0.129
0.26 r_0	-0.097	0.015	-0.464	0.617	-0.156
0.30 r_0	-0.095	0.018	-0.527	0.810	-0.185

Table 4: Expected value, standard deviation, skewness, kurtosis and coefficient of variation for the distributions of the nearest neighbour transfer integrals $J_{19,20}, J_{20,21}, \ldots, J_{27,19}$ connecting the nearest neighbour BChl molecules in B800 ring – uncorrelated Gaussian static disorder $\delta r_m (m = 1, \ldots, 27)$ in radial positions of BChl molecules; the strength of static disorder $\Delta_r \in \langle 0.02 r_0, 0.30 r_0 \rangle$.

interval $\Delta_r \in \langle 0.02 r_0, 0.30 r_0 \rangle$ (see Fig.7). The sign of α_4 is positive except the distribution of $J_{1,2}$ for the lowest static disorder strengths (see Table 1 – Table 4). Due to nonconstant expected values, influence of fluctuations δr_m to the distributions of $J_{1,2}$, $J_{1,19}$, $J_{2,19}$ and $J_{19,20}$ can be compared using the coefficient of variation *c*. The strongest influence can be seen in case of the distribution of $J_{1,2}$ and the weakest one in case of $J_{2,19}$ (see Table 1 – Table 4 and Fig.8).

5 Conclusions

Comparison of all four distributions obtained within static disorder in radial positions of BChl molecules can be summarized as follows. Expected values of the distributions of the nearest neighbour transfer integrals $J_{1,2}$, $J_{1,19}$, and $J_{19,20}$ depend on static disorder strength. Expected value of the distribution of $J_{2,19}$ is nearly constant.

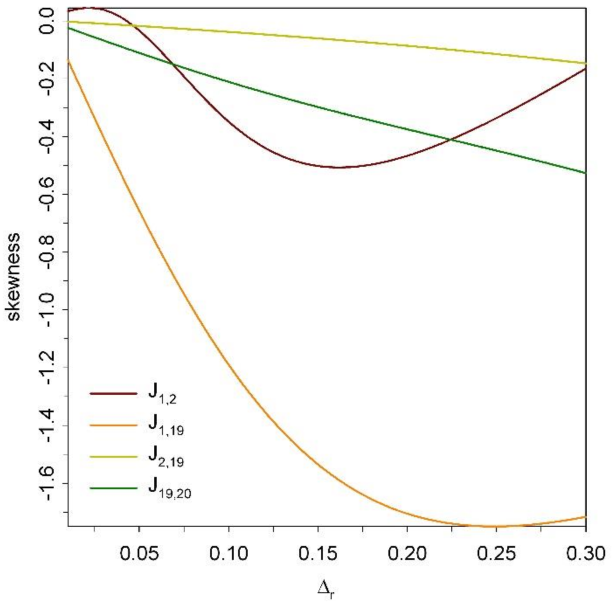

Fig. 6 The dependence of skewness α_3 on the static disorder strength Δ_r for all presented four types of distributions.

Fig.7 The dependence of kurtosis α_4 on the static disorder strength Δ_r for all presented four types of distributions.

All four distributions are skewed to left hand side. Through the comparison of coefficients of variation c we can conclude that static disorder in radial positions of BChl molecules mostly influences the transfer integrals $J_{1,2}$.

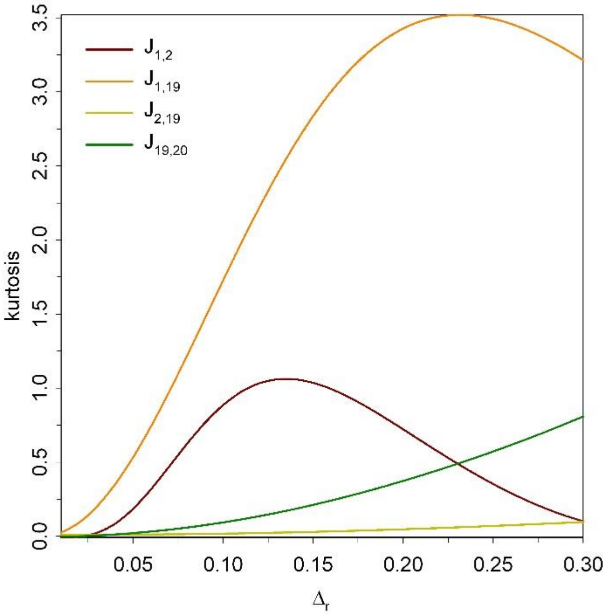

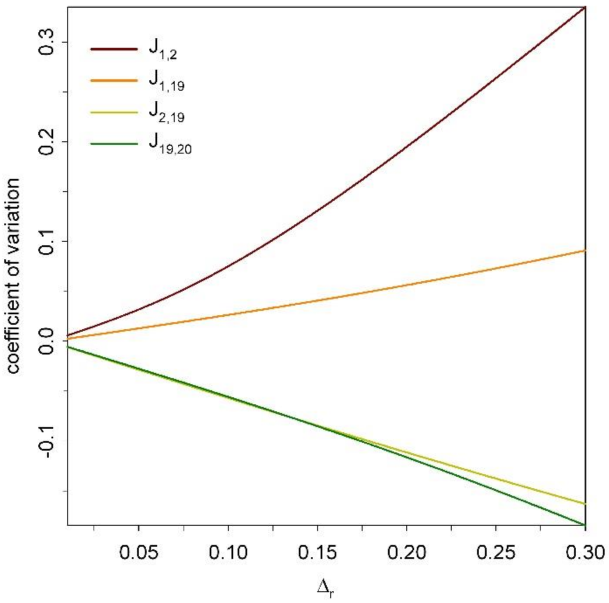

Fig.8 The dependence of coefficient of variation c on the static disorder strength Δ_r for all presented four types of distributions.

Acknowledgement:

Support from the Faculty of Science, University of Hradec Králové (project of specific research No. 2104/2017) is gratefully acknowledged.

References:

[1] D. W. Lawlor, *Photosynthesis*, Spriger, New York 2001.

[2] R. van Grondelle and V. I. Novoderezhkin, Energy transfer in photosynthesis: experimental

insights and quantitative models, *Phys. Chem. Chem. Phys.*, Vol.8, 2003, pp. 793–807.

[3] G. McDermott, et al., Crystal structure of an integral membrane light-harvesting complex from photosynthetic bacteria, *Nature*, Vol.374, 1995, pp. 517–521.

[4] M. Z. Papiz, et al., The structure and thermal motion of the B 800-B850 LH2 complex from Rps. acidophila at 2.0 A resolution and 100 K: new structural features and functionally relevant motions, *J. Mol. Biol.*, Vol.326, 2003, pp. 1523–1538.

[5] K. McLuskey, et al., The crystalographic structure of the B800–820 LH3 light-harvesting complex from the purple bacteria Rhodopseudomonas acidophila strain 7050, *Biochemistry*, Vol.40, 2001, pp. 8783–8789.

[6] W. P. F. de Ruijter, et al., Observation of the Energy–Level Structure of the Low–Light Adapted B800 LH4 Complex by Single–Molecule Spectroscopy, *Biophys. J.*, Vol.87, 2004, pp. 3413–3420.

[7] A.W. Roszak, et al., Crystal structure of the RCLH1 core complex from Rhodopseudomonas palustris, *Science*, Vol.302, 2003, pp. 1976–1972.

[8] R. Kumble and R. Hochstrasser, Disorder–induced exciton scattering in the light–harvesting systems of purple bacteria: Influence on the anisotropy of emission and band → band transitions, *J. Chem. Phys.*, Vol.109, 1998, pp. 855–865.

[9] V. Nagarajan, et al., Femtosecond pump–probe spectroscopy of the B850 antenna complex of Rhodobacter sphaeroides at room temperature, *J. Phys. Chem. B*, Vol.103, 1999, pp. 2297–2309.

[10] V. Nagarajan and W. W. Parson, Femtosecond fluorescence depletion anisotropy: Application to the B850 antenna complex of Rhodobacter sphaeroides, *J. Phys. Chem. B*, Vol.104, 2000, pp. 4010–4013.

[11] V. Čápek, I. Barvík and P. Heřman, Towards proper parametrization in the exciton transfer and relaxation problem: dimer, *Chem. Phys.*, Vol.270, 2001, pp. 141–156.

[12] P. Heřman and I. Barvík, Towards proper parametrization in the exciton transfer and relaxation problem. II. Trimer, *Chem. Phys.*, Vol.274, 2001, pp. 199–217.

[13] P. Heřman, I. Barvík and M. Urbanec, Energy relaxation and transfer in excitonic trimer, *J. Lumin.*, Vol.108, 2004, pp. 85–89.

[14] [14] P. Heřman, et al., Exciton scattering in light–harvesting systems of purple bacteria, *J. Lumin.*, Vol.94–95, 2001, pp. 447–450.

[15] P. Heřman and I. Barvík, Non–Markovian effects in the anisotropy of emission in the ring antenna subunits of purple bacteria photosynthetic systems, *Czech. J. Phys.*, Vol.53, 2003, pp. 579–605.

[16] P. Heřman, et al., Influence of static and dynamic disorder on the anisotropy of emission in the ring antenna subunits of purple bacteria photosynthetic systems, *Chem. Phys.*, Vol.275, 2002, pp. 1–13.

[17] P. Heřman and I. Barvík, Temperature dependence of the anisotropy of fluorescence in ring molecular systems, *J. Lumin.*, Vol.122–123, 2007, pp. 558–561.

[18] P. Heřman, D. Zapletal and I. Barvík, Computer simulation of the anisotropy of fluorescence in ring molecular systems: Influence of disorder and ellipticity, *Proc. IEEE 12th Int. Conf. on Computational Science and Engineering*, Vancouver: IEEE Comp. Soc., 2009, pp. 437–442.

[19] P. Heřman and I. Barvík, Coherence effects inring molecular systems, *Phys. Stat. Sol. C*, Vol.3, 2006, 3408–3413.

[20] P. Heřman, D. Zapletal and I. Barvík, The anisotropy of fluorescence in ring units III: Tangential versus radial dipole arrangement, *J. Lumin.*, Vol.128, 2008, pp. 768–770.

[21] P. Heřman, I. Barvík and D. Zapletal, Computer simulation of the anisotropy of fluorescence in ring molecular systems: Tangential vs. Radial dipole arrangement, *Lecture Notes in Computer Science*, Vol.5101, 2008, pp. 661–670.

[22] P. Heřman, D. Zapletal and I. Barvík, Lost of coherence due to disorder in molecular rings, *Phys. Stat. Sol. C*, Vol.6, 2009, pp. 89–92.

[23] P. Heřman, D. Zapletal and J. Šlégr, Comparison of emission spectra of single LH2 complex for different types of disorder, *Phys. Proc.*, Vol.13, 2011, pp. 14–17.

[24] D. Zapletal and P. Heřman, Simulation of molecular ring emission spectra: localization of exciton states and dynamics, *Int. J. Math. Comp. Sim.*, Vol.6, 2012, pp. 144–152.

[25] M. Horák, P. Heřman and D. Zapletal, Simulation of molecular ring emission spectra – LH4 complex: localization of exciton states and dynamics, *Int. J. Math. Comp. Sim.*, Vol.7, 2013, pp. 85–93.

[26] P. Heřman and D. Zapletal, Intermolecular emission spectra for LH4 ring, *Int. J. Math. Comp. Sim.*, Vol.7, 2013, pp. 249–257.

[27] M. Horák, P. Heřman and D. Zapletal, Modeling of emission spectra for molecular rings – LH2, LH4 complexes, *Phys. Proc.*, Vol.44, 2013, pp. 10–18.

[28] P. Heřman, D. Zapletal and M. Horák, Emission spectra of LH2 complex: full Hamiltonian model, *Eur. Phys. J. B,* Vol.86, 2013, art. no. 215.

[29] P. Heřman and D. Zapletal, Emission Spectra of LH4 Complex: Full Hamiltonian Model, *Int. J. Math. Comp. Sim.*, Vol. 7, 2013, pp. 448–455.

[30] P. Heřman and D. Zapletal, Simulation of Emission Spectra for LH4 Ring: Intermolecular Coupling Fluctuation Effect, *Int. J. Math. Comp. Sim.*, Vol.8, 2014, pp. 73–81.

[31] D. Zapletal and P. Heřman, Photosynthetic complex LH2 – Absorption and steady state fluorescence spectra, *Energy*, Vol.77, 2014, pp. 212–219.

[32] P. Heřman and D. Zapletal, Simulations of emission spectra for LH4 Ring – Fluctuations in radial positions of molecules, *Int. J. Biol. Biomed. Eng.*, Vol.9, 2015, pp. 65–74.

[33] [33] P. Heřman and D. Zapletal, Computer simulation of emission and absorption spectra for LH2 ring, *Lecture Notes in Computer Science*, Vol.343, 2015, pp. 221–234.

[34] P. Heřman and D. Zapletal, Modeling of Absorption and Steady State Fluorescence Spectra of Full LH2 Complex (B850 – B800 Ring), *Int. J. Math. Mod. Meth. Appl. Sci.*, Vol.9, 2015, pp. 614–623.

[35] P. Heřman and D. Zapletal, Modeling of Emission and Absorption Spectra of LH2 Complex (B850 and B800 Ring) – Full Hamiltonian Model, *Int. J. Math. Comp. Sim.*, Vol.10, 2016, pp. 208–217.

[36] P. Heřman and D. Zapletal, B–α/B–β Ring from Photosynthetic Complex LH4, Modeling of Absorption and Fluorescence Spectra, *Int. J. Math. Comp. Sim.*, Vol.10, 2016, pp. 332–344.

[37] P. Heřman and D. Zapletal, B850 Ring from Photosynthetic Complex LH2 - Comparison of Different Static Disorder Types, *Int. J. Math. Comp. Sim.*, Vol.10, 2016, pp. 361–369.

[38] P. Heřman and D. Zapletal, Fluctuations of Bacteriochlorophylls Positions in B850 Ring from Photosynthetic Complex LH2 *Int. J. Math. Comp. Sim.*, Vol.10, 2016, pp. 381–389.

[39] P. Heřman, et al., Fluctuations of Pigments Dipole Moment Orientations in B850 Ring from Photosynthetic Complex LH2, *WSEAS Trans. App. Theor. Mech.*, Vol.12, 2017, pp. 105–112.

[40] P. Heřman, I. Barvík and D. Zapletal, Energetic disorder and exciton states of individual molecular rings, *J. Lumin.*, Vol.119–120, 2006, pp. 496–503.

[41] C. Hofmann, T. J. Aartsma and J. Köhler, Energetic disorder and the B850–exciton states of individual light–harvesting 2 complexes from Rhodopseudomonas acidophila, *Chem. Phys. Lett.*, Vol.395, 2004, pp. 373–378